Organic & Biomolecular Chemistry

Accepted Manuscript

ROYAL SOCIETY OF CHEMISTRY

www.rsc.org/obc

Journal Name

RSCPublishing

COMMUNICATION

Cite this: DOI: 10.1039/xoxxoooooox

Absolute Configuration of Remisporines A & B

Edward C. Sherer*[a] , James R. Cheeseman[b], R. Thomas Williamson[c]

Received ooth January 2012,
Accepted ooth January 2012

DOI: 10.1039/xoxxoooooox

www.rsc.org/

The absolute configuration of remisporine B was determined based on a comparison of experimental and calculated electronic circular dichorism (ECD) spectra. Density functional theory (DFT) was used to calculate the ECD spectra varying the parameter controlling the number of calculated electronic transitions. Mapping the reaction surface provided support for the proposed Diels-Alder dimerization of remisporine A to form remisporine B.

Introduction

Remisporine A (**1**, Scheme 1), is a fungal metabolite originally isolated from a liquid culture of the marine fungus *Remispora maritima*.[1] Remisporine A was found to be unstable and was shown to autocatalytically dimerize in solution to produce remisporine B, a stereospecific product, via a presumed Diels–Alder reaction. The structure of remisporine B was originally characterized by detailed NMR studies that also revealed its relative stereochemistry (**2**, Scheme 1).[1] An electronic circular dichroism (ECD) spectrum was obtained but at the time of the original work, technology to develop an accurate calculated spectrum for determining the absolute configuration did not exist and the molecule was arbitrarily assigned as shown (**2**) in Scheme 1. In this work, we show that modern density functional theory (DFT) methods can construct a reliable and satisfying match to the experimental data that assigns the absolute configuration (**3**, Scheme 1). In addition, we show that an overall exothermic cascade coupled with a reasonable Diels-Alder cyclization barrier supports the proposed mechanism for formation of remisporine B.

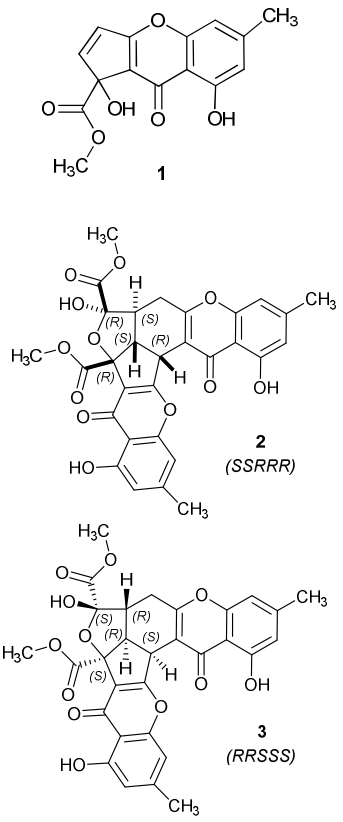

Scheme 1

Methods

DFT calculations were performed using Gaussian09.[2] Conformational space was exhaustively sampled using three conformer generators (rules-based generation relying on sampling if favorable torsion profiles and random displacement which does not consider favorable torsions during generation but for which subsequent energy minimizations are required) followed by molecular mechanics minimization using MMFF94, a workflow that has been previously published.[3] DFT with the B3LYP functional[4] and the 6-31G** basis set[5-7] was used to identify the lowest energy conformers contributing to the Boltzmann distributions for each structure at 298.15 K. All stationary points were confirmed with frequency calculations. To calculate ECD spectra, B3LYP geometries were used as input for calculations using the 6-31++G**[8,9] basis set either *in vacuo* or in an implicit solvent using Cramer and Truhlar's SMD continuum solvation methodology

(solvent = methanol).[10] Only conformers that contributed more than 1.0% to the total *in vacuo* conformer distribution were sent for implicit solvation minimization or calculation of ECD spectra. Time-dependent (TD-DFT) methodology[11] was employed using the keywords: TD=full,singlet with NSTATES=20, 50, or 100, and integral=ultrafinegrid (the default value of NSTATES in Gaussian is 3). Spectra were displayed using SpecDis.[12,13] We used a σ = 0.16 or 0.30 eV for band broadening in this work. Final weighting of the conformer specific ECD spectra was done using the calculated Boltzmann population.

Exploration of solvent complexation of **2** to investigate the effect of explicit solvation on the calculated ECD spectra was accomplished using molecular dynamics simulations run with Desmond.[14-16] An explicit solvent box of methanol was used according to default parameters and a 50 ns simulation was run within the NPT ensemble. Hydrogen bonded solvent molecules were monitored over the course of the trajectory. Snapshots output from the trajectory representing the maximum first shell solvation were used as input for DFT ECD spectra calculations. The explicit complexes were minimized both *in vacuo* and in implicit methanol.

Characterization of the proposed reaction mechanism was performed using the M062X[17] density functional and the 6-31+G** basis set. All stationary points and transition structures were confirmed with frequency calculations (single imaginary vibration for transition states, and no imaginary vibrations for minima). Free energies were calculated at 298K. Transition states for the Diels-Alder step were treated as open-shell singlets and represented a concerted, though highly asynchronous, pathway. Transition states were treated as restricted, and IRC calculations from the transition state described smoothly connected to reactants and products. No intermediate structure was identified that would support a step-wise mechanism. Basis set superposition error (BSSE) correction was not applied.

Results and Discussion

Questions of absolute configuration at Merck Research Laboratories are addressed by the Stereochemical Assignment Task Force (SATF), a multi-disciplinary team composed of synthetic and analytical chemists from the fields of NMR, X-ray crystallography, IR, VCD, and computational chemistry.[3] Parallel efforts across these disciplines have enabled the routine assignment of absolute configuration for a wide array of complex molecules. When enough sample is available, the method of choice is VCD, owing to its speed, accuracy, and generally unambiguous result. In the case of **2**, no sample was available for analysis. Calculation of ECD spectra is more complex owing to the increased complexity (in computational cost and accuracy) of calculating electronic transitions. The predicted ECD spectra are more dependent on method and basis set combinations, but experience indicates that the method selected here should be sufficient.[18,19] Comparison of the calculated ECD spectra to the previously published ECD spectrum of **2** or **3** (ambiguity exists in which enantiomer was originally measured and reported[1]) is possible and forms the basis of our revised assignment (the original measured ECD spectrum is contained in citation 5 of Kong and Carter[1]).

Figure 1 shows the measured ECD spectrum for **2** or **3** measured in methanol. While the assignment of relative configuration was made by NMR, assignment of the absolute configuration by Kong and Carter was arbitrary.[1] The published spectrum and the mirrored enantiomeric spectrum are shown overlaid. Calculation of the ECD spectrum for the two enantiomers should allow for unambiguous assignment of absolute configuration.

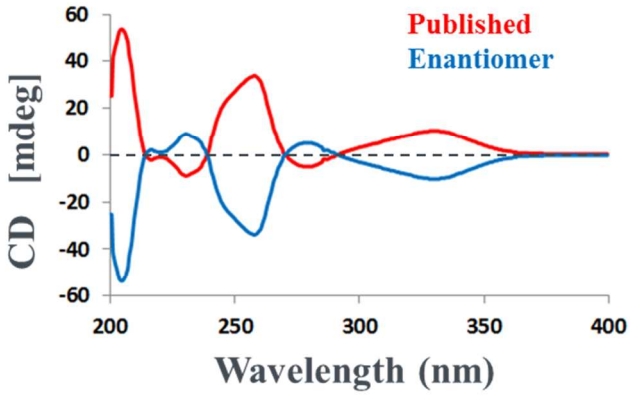

Figure 1: CD spectrum of **2** or **3** (1.5 mg in 2 mL MeOH)[1]

Calculation of ECD spectra for molecule **2** required substantial computational resources and long compute times. Increasing the number of electronic states calculated leads to increased computational expense, and owing to limitations in resources, the number of states (NSTATES=N) is commonly set to ≤ 20. With a smaller number of calculated states caution must be used when assigning absolute configuration since it can be possible to shift the calculated spectrum (of either enantiomer) along the wavelength axis such that the experimental spectrum might match either enantiomer equally well. This arises from the need to commonly shift or scale the calculated frequency range to optimally match experiment. Here we note that a more complete (filling in at lower wavelengths) calculated ECD spectrum can remove this ambiguity.

In vacuo conformer searches led to four predominant conformations for **2** as depicted in Figure 2. The Boltzmann-weighted spectrum is generated from a linear combination of the four calculated ECD curves. Initial matching of the spectra using NSTATES=20 indicated poor confidence in the absolute configuration assignments (Figure S1, Supporting Information). Smoothing of the discreet calculated peaks using band broadening provides the overall ECD spectrum; this smoothing is governed by the σ factor set to a default value of 0.16. Increasing σ to a value of 0.30 leads to a more smoothed surface which better approximates the curvature of the measured spectrum. Smoothing accounts for conformational diversity, solvent effects, and artifacts in geometry arising from assuming ground state geometries for the excited states. Discreet peaks allow for an easy comparison of spectra generated from different computational methods or when comparing spectra and intensities derived from increasing the number of sampled electronic transitions. Figure S1 provides the *in vacuo* and implicit methanol calculated ECD using NSTATES=20, 50, and 100 states. Since the experimental spectrum went down to 200 nm, it was not until rather higher values of NSTATES was used that the entire measured spectrum was reproduced computationally. Increasing the number of calculated transitions to better approximate the full range of an experimental ECD has been reported

previously.[20,21] A small number of calculated electronic states initially populates lower energy transitions which have longer wavelengths, and in order to reach to the lower end of the experimental spectrum at 200nm, the electronic transitions are higher in energy and for this reason the number of states must be increased significantly. Owing to the large size of the molecule, there are a large number of electronic transitions relative to smaller organic molecules routinely analyzed using ECD. In moving from 20 to 100 states, the distribution of transitions at lower wavelength increases, and dramatically influences the relative intensities of dominant peaks in the spectrum leading to better agreement in the match to experiment. The most dominant feature in the spectrum is the peak at approximately 203nm which is an n→π* transition from the cyclopenta[*b*]chromen-9(1H)-one ketone oxygen of the ring to the opposite cyclopenta[*b*]chromen-9(1H)-one ring, and is not identified until excited state 61 out of 100.

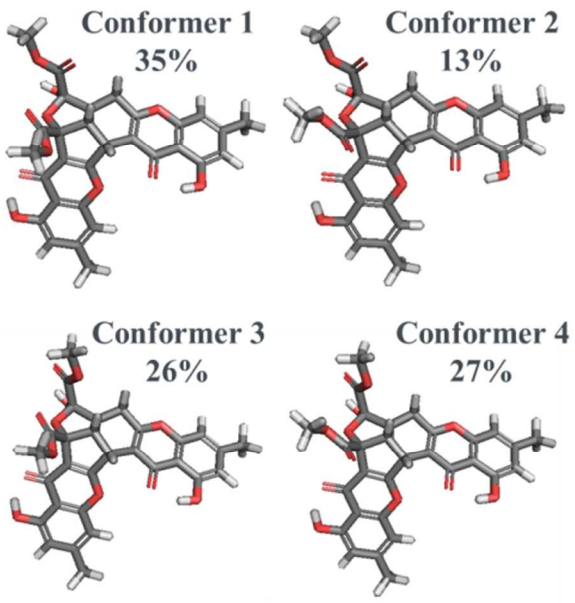

Figure 2. Dominant energy minimized conformations (*SSRRR*) of **2** contributing to the Boltzmann population indicating flexibility of ester tails.

When the calculated ECD spectra are overlaid (Figure 3) onto the published ECD for proposed enantiomer **2** or enantiomer **3**, it is apparent that the assigned configuration should be *(RRSSS)* as depicted in Scheme 1 for **3** and not *(SSRRR)* for **2** as originally proposed by Kong and Carter.[1] A comparison of the *in vacuo* ECD spectra and the implicit methanol spectra indicates good agreement.

Since there is a significant concentration of hydrogen bond donors on **2**, we pursued the identification of a solvated complex to determine the effect of explicit solvation on the calculated ECD. Molecular dynamics simulations were run in explicit methanol to determine optimal first shell solvation. The number of directed hydrogen bonds between solvent and **2** over the course of the trajectory peaked at nine. For this reason, diverse snapshots were extracted from the trajectory where nine solvent molecules were coordinated to **2**. These snapshots were minimized with B3LYP and energetic comparison led to one dominant solvated structure depicted in Figure 4.

Figure S2 compares the calculated ECD for the *in vacuo* explicitly solvated complex, and the explicit solvent complex further minimized within implicit methanol (both calculated using NSTATES=100). Increasing NSTATES to 200 for the *in vacuo* explicit solvent complex led to an identical calculated ECD as that for NSTATES=100 (data not shown).

Calculated ECD derived from modelling **2** *in vacuo*, using implicit methanol, adding explicit methanol solvation, or modelling the explicit complex in implicit methanol were all in good agreement.

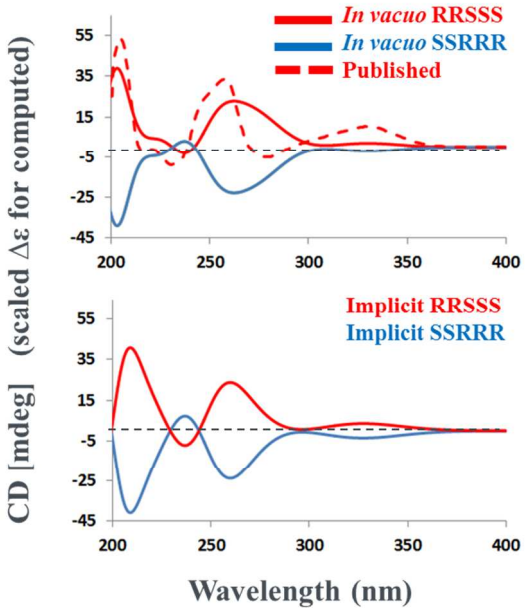

Figure 3. *In vacuo* and implicit methanol calculated ECD (NSTATES=100) for the two enantiomers **2** and **3** overlaid onto the experimental spectrum. The value for σ = 0.30 was chosen to better approximate the curvature of the experimental data.

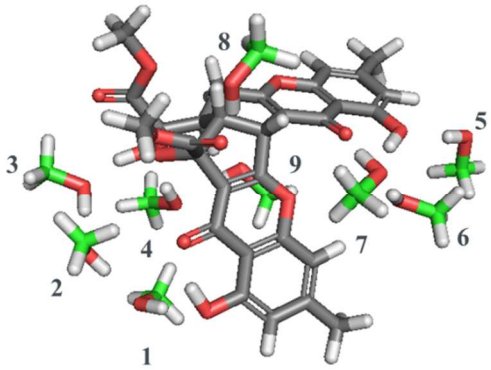

Figure 4. Explicit solvation of (*SSRRR*) **2** (grey) with nine methanol molecules (green).

The proposed reaction mechanism (Scheme 2) was investigated with the M062X density functional using a moderately sized basis set 6-31+G** and B3LYP/6-31G**. Publications by

Houk and Cramer indicate that these DFT methods should be sufficient for interpreting Diels-Alder transition states and energetics.[22,23] Free energy values included in the following text are M062X/6-31+G** (see Supporting Information for details and B3LYP numbers). The Diels-Alder reaction is calculated to have an activation free energy barrier (*in vacuo*) of 15.2 kcal/mol with an exothermic free energy of reaction moving from **1** to **4** of -29.0 kcal/mol. The reaction is slightly endothermic, moving through the retro-Aldol conversion to **5** at 5.8 kcal/mol. Aromatization from **5** to **6** is exothermic at -23.2 kcal/mol, with the final cyclization to form **2** being endothermic by 2.2 kcal/mol.

The transition state for the proposed cyclization of **1** to **4** is provided in Figure 5.[1] A calculated barrier of ~15 kcal/mol for the initial Diels-Alder cyclization is quite low, and well within the normal ranges for this type of reaction (e.g., the Diels-Alder closure of butadiene + ethylene is 27.5 kcal/mol[24-26]). Electronic reaction energies calculated with B3LYP are similar to the M062X values, and owing to little charge build up in the transition state, implicit solvation did not change the B3LYP barrier height significantly (ΔG difference of -1.5 kcal/mol). We attribute a rather large difference between the free energy barriers calculated using B3LYP and M062X to the better treatment of dispersion effects which are significant in the stacked pre-transition state complex and the transition state itself (leading to a difference of ~10-12 kcal/mol). These differences were further investigated by mapping the first step in the proposed mechanism using three additional DFT methods: CAM-B3LYP[27] long range correction, B3LYP with D2[28] with dispersion correction, and D3[29] dispersion and damping corrections (Supporting Information). With a better treatment of dispersion effects, the D2 and D3 corrected energies show favorable energetics of forming the van der Waals complex similar to M062X.

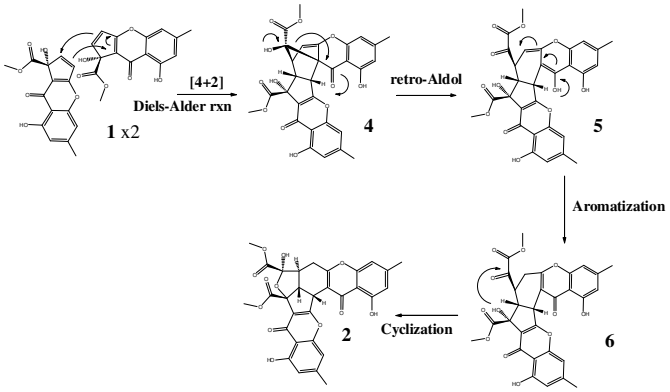

Scheme 2

Determining that the proposed Diels-Alder reaction pathway is reasonable does not determine absolute configuration, however, Diels-Alder reactions are known to impart a high degree of stereo- and regio-selectivity.[30-32] While a series of calculations to gauge the facial and *endo/exo* selectivity of the Diels-Alder step is of interest and would lend support to the final relative configuration, the computational cost limits our further pursuit of these calculations.

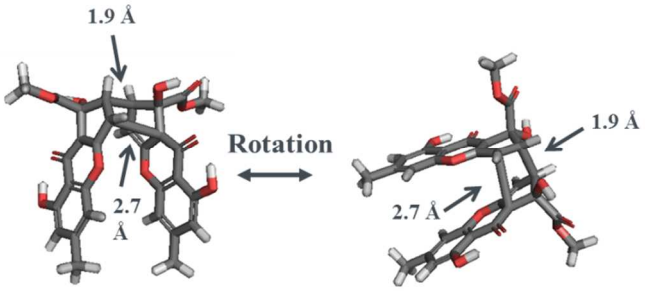

Figure 5: Transition state for the Diels-Alder cyclization of **1** to **4** calculated at the M062X/6-31+G** level (*SSRRR*).

Conclusions

Calculation of ECD spectra has indicated that the absolute configuration depicted for **2** in the original publication of the structure of remisporine B needs to be revised. By explicitly calculating the ECD spectra for **2** and **3** we have shown that the absolute configuration of remisporine B is *(RRSSS)* as depicted in Scheme 1 for **3.** The overall exothermic nature of the proposed reaction mechanism and the reasonable barrier to Diels-Alder cyclization is consistent with the originally proposed mechanism for the autocatalytic dimerization of remisporine A to form remisporine B. Based on these conclusions, the actual absolute stereochemistry of remisporine A (**7**, Scheme 3) should be assigned accordingly as *S*.

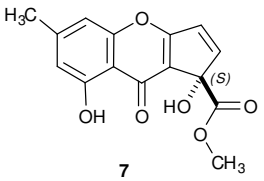

7

Scheme 3

Notes and references

[a] Structural Chemistry, Merck Research Labs, 126 E. Scott Avenue, Rahway, NJ 07065.
[b] Gaussian, Inc. 340 Quinnipiac St Bldg 40, Wallingford, CT 06492.
[c] NMR Structure Elucidation Group, Process & Analytical Chemistry, Merck Research Labs, 126 E. Scott Avenue, Rahway, NJ 07065.

Electronic Supplementary Information (ESI) available: B3LYP and M062X reaction pathways (electronic and free energies). CAM-B3LYP calculated ECD example. Calculated ECD using NSTATES=20,50,100. Table of DFT estimates for first step in mechanism. Coordinates for all minima and transition states reported in this manuscript.

Acknowledgements: We thank Fernando Clemente for helpful discussions concerning the computational work. We thank Gary Martin for helpful comments during manuscript preparation.

References

1. F.M. Kong, and G.T. Carter, *Tetrahedron Letters,* 2003, **44**(15), 3119.
2. M.J. Frisch, G.W. Trucks, H.B. Schlegel, G.E. Scuseria, M.A. Robb, J.R. Cheeseman, G. Scalmani, V. Barone, B.

Mennucci, G.A. Petersson, H. Nakatsuji, M. Caricato, X. Li, H.P. Hratchian, A.F. Izmaylov, J. Bloino, G. Zheng, J.L. Sonnenberg, M. Hada, M. Ehara, K. Toyota, R. Fukuda, J. Hasegawa, M. Ishida, T. Nakajima, Y. Honda, O. Kitao, H. Nakai, T. Vreven, J. Montgomery, J.A., J.E. Peralta, F. Ogliaro, M. Bearpark, J.J. Heyd, E. Brothers, K.N. Kudin, V.N. Staroverov, R. Kobayashi, J. Normand, K. Raghavachari, A. Rendell, J.C. Burant, S.S. Iyengar, J. Tomasi, M. Cossi, N. Rega, J.M. Millam, M. Klene, J.E. Knox, J.B. Cross, V. Bakken, C. Adamo, J. Jaramillo, R. Gomperts, R.E. Stratmann, O. Yazyev, A.J. Austin, R. Cammi, C. Pomelli, J.W. Ochterski, R.L. Martin, K. Morokuma, V.G. Zakrzewski, G.A. Voth, P. Salvador, J.J. Dannenberg, S. Dapprich, A.D. Daniels, Ö. Farkas, J.B. Foresman, J.V. Ortiz, J. Cioslowski, and D.J. Fox. Gaussian 09, Revision A.02. Wallingford, CT: Gaussian, Inc.; 2009.

3. E.C. Sherer, C.H. Lee, J. Shpungin, J.F. Cuff, C.X. Da, R. Ball, R. Bach, A. Crespo, X.Y. Gong, and C.J. Welch, *Journal of Medicinal Chemistry,* 2014, **57**(2), 477.
4. C.T. Lee, W.T. Yang, and R.G. Parr, *Physical Review B,* 1988, **37**(2), 785.
5. R. Ditchfield, W.J. Hehre, and J.A. Pople, *Journal of Chemical Physics* 1971, **54**(2), 724.
6. P.C. Hariharan, and J.A. Pople, *Theoretica Chimica Acta,* 1973, **28**(3), 213.
7. W.J. Hehre, R. Ditchfield, and J.A. Pople, *Journal of Chemical Physics,* 1972, **56**(5), 2257.
8. T. Clark, J. Chandrasekhar, G.W. Spitznagel, and P.V. Schleyer, *Journal of Computational Chemistry,* 1983, **4**(3), 294.
9. M.J. Frisch, J.A. Pople, and J.S. Binkley, *Journal of Chemical Physics,* 1984, **80**(7), 3265.
10. A.V. Marenich, C.J. Cramer, and D.G. Truhlar, *Journal of Physical Chemistry B,* 2009, **113**(18), 6378.
11. R. Bauernschmitt, and R. Ahlrichs, *Chemical Physics Letters,* 1996, **256**(4-5), 454.
12. T. Bruhn, A. Schaumloffel, Y. Hemberger, and G. Bringmann, *Chirality,* 2013, **25**(4), 243.
13. G. Mazzeo, E. Santoro, A. Andolfi, A. Cimmino, P. Troselj, A.G. Petrovic, S. Superchi, A. Evidente, and N. Berova, *Journal of Natural Products,* 2013, **76**(4), 588.
14. Schrödinger Release 2014-1: Maestro-Desmond Interoperability Tools, version 3.7. New York, NY: Schrödinger; 2014.
15. Schrödinger Release 2014-1: Desmond Molecular Dynamics System, version 3.7. New York, NY: Research DES; 2014.
16. K.J. Bowers, E. Chow, H. Xu, R.O. Dror, M.P. Eastwood, B.A. Gregersen, J.L. Klepeis, I. Kolossvary, M.A. Moraes, F.D. Sacerdoti, J.K. Salmon, Y. Shan, and D.E. Shaw. Scalable Algorithms for Molecular Dynamics Simulations on Commodity Clusters. Proceedings of the ACM/IEEE Conference on Supercomputing (SC06). Tampa, Fl; 2006.
17. Y. Zhao, and D.G. Truhlar, *Theoretical Chemistry Accounts,* 2008, **120**(1-3), 215.
18. P.J. Stephens, D.M. McCann, E. Butkus, S. Stoncius, J.R. Cheeseman, and M.J. Frisch, *Journal of Organic Chemistry,* 2004, **69**(6), 1948.
19. P.J. Stephens, D.M. McCann, F.J. Devlin, J.R. Cheeseman, and M.J. Frisch, *Journal of the American Chemical Society,* 2004, **126**(24), 7514.
20. F. Cherblanc, Y.P. Lo, E. De Gussem, L. Alcazar-Fuoli, E. Bignell, Y.A. He, N. Chapman-Rothe, P. Bultinck, W.A. Herrebout, R. Brown, H.S. Rzepa, and M.J. Fuchter, *Chemistry-a European Journal,* 2011, **17**(42), 11868.
21. M. Adrian-Scotto, S. Antonczak, J.H. Bredehoft, S.V. Hoffmann, and U.J. Meierhenrich, *Symmetry,* 2010, **2**(2), 935.
22. A.N. Garr, D.H. Luo, N. Brown, C.J. Cramer, K.R. Buszek, and D. VanderVelde, *Organic Letters,* 2010, **12**(1), 96.
23. R.S. Paton, J.L. Mackey, W.H. Kim, J.H. Lee, S.J. Danishefsky, and K.N. Houk, *Journal of the American Chemical Society,* 2010, **132**(27), 9335.
24. L.R. Domingo, and J.A. Saez, *Organic & Biomolecular Chemistry,* 2009, **7**(17), 3576.
25. E. Goldstein, B. Beno, and K.N. Houk, *Journal of the American Chemical Society,* 1996, **118**(25), 6036.
26. D. Rowley, and H. Steiner, *Discussions of the Faraday Society,* 1951, **10**, 198.
27. T. Yanai, D.P. Tew, and N.C. Handy, *Chemical Physics Letters,* 2004, **393**(1-3), 51.
28. S. Grimme, J. Antony, S. Ehrlich, and H. Krieg, *Journal of Chemical Physics,* 2004, **132**(15), 154104.
29. S. Grimme, *Journal of Computational Chemistry,* 2006, **27**(15), 1787.
30. G. Brieger, and J.N. Bennett, *Chemical Reviews,* 1980, **80**(1), 63.
31. J.G. Martin, and R.K. Hill, *Chemical Reviews,* 1961, **61**(6), 537.
32. W.R. Roush, M. Kageyama, R. Riva, B.B. Brown, J.S. Warmus, and K.J. Moriarty, *Journal of Organic Chemistry,* 1991, **56**(3), 1192.